Journal of Information Hiding and Multimedia Signal Processing ©2017 ISSN 2073-4212
Ubiquitous International Volume **8**, Number **4**, July **2017**

Vessel Detection in Chicken Chorioallantoic Membrane Image

Chin-Chen Chang

Department of Information Engineering and Computer Science
Feng Chia University
100, Wenhwa Rd., Seatwen, Taichung 40724, Taiwan, R.O.C
alan3c@gmail.com

Pei-Yan Pai

Department of Computer Science
National Tsing-Hua University
101, Kuang Fu Rd, Sec.2, HsingChu, Taiwan 300 R.O.C
d938338@oz.nthu.edu.tw

Meng-Hsiun Tsai and Yung-Kuan Chan

Department of Management Information Systems
National Chung Hsing University
250, Kuokuang Rd., Taichung, Taiwan, R.O.C.
mht@nchu.edu.tw; ykchan@nchu.edu.tw

Received March, 2013; revised December, 2014

Abstract. *Cancer is one of the top ten fatal diseases and scholars found out that the disease is related to Angiogenesis. People can know their disorder conditions and covering process by detecting features of their vessel area and track density. In this paper, we present an automatic method for vessel detection, called "Canny-Based Vessel Detector." At first, Canny edge detector is used to find out the edges of vessels. Next, vessels can be detected by observing the vessel colors and the changes of standard deviation around the vessels. The experimental results illustrate that the Canny-Based Vessel Detector can detect most of vessels in spite of a little part without discontinuation and ineffectiveness in very tiny vessels.*
Keywords: Angiogenesis, Canny edge detector, Standard deviation, Vessel segmentation

1. **Introduction.** The growth of new tissues relies on appropriate vassal through which nutrients are shipped and refuse excluded. The generation of new vessels, called Angiogenesis [7], is necessarily demanded for wound healing, tissue regeneration, reproduction, or growing [7]. In general, angiogenic growth factors will be released around the hurt or pathological tissues [12]. After the combination of the factors and receptors on endothelial cells these cells will be activated to secrete some of particular enzyme and growth factors, which dissolve the basement membrane on the original vessels so that those cells can divert the injured tissues to produce Angiogenesis whose regulation between vessel genesis and suppression is found to play an impressive role on disease healing [4, 6].

Angiogenesis is a required process in normal physiological change [7]. Moreover, scientists have discovered that the appearance of many diseases is concerned with it [4].

Either excessive or insufficient Angiogenesis can result in diseases [2]. Diabetic Retinopathy, Age-related macular degeneration, Rheumatoid arthritis, Kaposis sarcoma, Psoriasis, and so on are diseases indicating the phenomenon of excessive Angiogenesis. In addition, Angiogenesis plays an important role in generation, degeneration, and metastasis of tumor cells in want of vessels through which nutrient and oxygen are supplied [4, 5, 7, 8].

Tumor cells firstly release growth factors around near organizations to trigger residential health vessels to sprout new vessels in tumor. Once tumor is penetrated by new vessels, it will become larger quickly and then invade partial organs. Finally, other organs are invaded to form metastases [3, 7]. On the contrary, tumor cells will vanish without supply of blood. Hence, a great many scholars have started to discover anti-angiogenesis agents to suppress the activity of Angiogenesis such that the vessels around tumor cannot regenerate because of insufficient nutrient [9, 13].

Using rapidly formed chicken chorioallantoic membrane incapable of metabolism to observe the effect of medication on vessel formation is a kind of semi in vivo trial, called chicken chorioallantoic membrane assay, through which we can simulate how tumor triggers vessel proliferation. The assay is done in the early stages of fertilized chicken chorioallantoic membrane because vessel proliferation works like vessel proliferation triggered by tumor and both are very lively, so it is very suitable for simulating. Nowadays, there are many substances used to restrain vessels from generating. For example, Suramin can be adopted to prevent bFGF and its receptors from combination and then prohibit Angiogenesis. In this paper, chicken chorioallantoic membrane assay with aid of Surmain gives us an insight into the inhibitive ability of test medicine B against Angiogenesis. The test medicine is a kind of traditional Chinese medicine used to prohibit tumor cells from growing. The following shows the materials, equipment, and procedures, which are used in our experiments:

Materials:

Fertilized egg
Germfree filter paper (0.22um)
Test Medicine B
Suramin

Equipments:

A box for cell cultivation
A microscope
A camera

Procedures:

1. Place fertilized egg into the cultivation box for 7 days.
2. Open a hole on the blunt end of the egg.
3. Add PBS (200ul) into the chicken chorioallantoic membrane, and then tear the egg membrane carefully by tweezers. Don't destroy the vessels in the membrane.
4. With care, put those membrane filtrations stained with PBS, test Medicine B, and Suramin, respectively, in different chorioallantoic membrane vessels, use membrane filtrations (0.22 μm) and athletic tapes to enclose the hole on the egg, and place it back into the cultivation box with 37°C and 60% moisture for 24 hours.
5. After 24 hours, open the hole carefully. Don't destroy the vessels in the membrane and take a figure of it.
6. Calculate the status of vessel proliferation by using the Box-Counting Dimension of Fractal Analysis.

Vessel distribution, which is a kind of fractal analysis, is suitable for analyzing the density of vessel distribution. Locate vessel pattern on grids with identical size, calculate

the number of the grids through which vessels flow, and finally compute its $\boldsymbol{BCD}$ (Box-Counting Dimension) [11] whose definition follows:

$$\boldsymbol{BCD} = \frac{\boldsymbol{logN(E)}}{\boldsymbol{log(\frac{1}{E})}}. \tag{1}$$

Figure 1 shows $\mathbf{5 \times 5}$ grids with edge size $\boldsymbol{E = 1/5}$ where the number of the grids through which vessels flow is $\boldsymbol{N(E) = 11}$ and $\boldsymbol{BCD = 1.49}$. The less the value of $\boldsymbol{BCD}$ is, the less the density of vessel distribution will be. Accordingly, $\boldsymbol{BCD}$ can be used to analyze the density of vessel distribution.

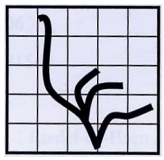

FIGURE 1. Grids with fractal analysis

The experimental results and their $\boldsymbol{BCD}$ are shown in Figures 2, and 3, respectively. Figure 2(a) illustrates the chicken chorioallantoic membrane image mixed with PBS, which is a normal chicken chorioallantoic membrane image. Figure 2(b) and (c) are the normal chicken chorioallantoic membrane image mixed with Test Medicine B and the one mixed with suramin, respectively. The $\boldsymbol{BCD}$ of chicken chorioallantoic membrane mixed with suramin and that with Test Medicine B are shown in Figure 3, illustrating that the $\boldsymbol{BCD}$ on the normal chicken chorioallantoic membrane image is much less than that in the image mixed with Test Medicine B or with suramin. In addition, the $\boldsymbol{BCD}$ on the image mixed with Test Medicine B is more than that on the image mixed with suramin. The experimental results show that Test Medicine B is more powerful in anti-angiogenesis than suramin does.

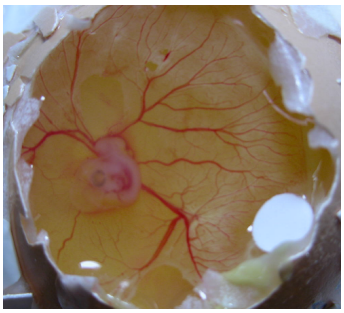

(a) The image mixed with PBS

(b) The image mixed with B

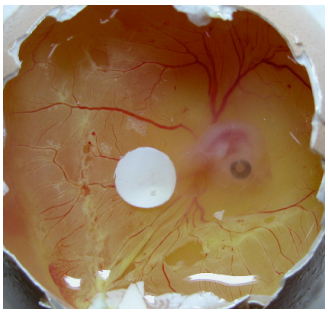

(c) The image mixed with suramin

FIGURE 2. The experimental results

With experimental results, it is shown that chicken chorioallantoic membrane assay can be used to examine whether a medicine can be used to trigger or suppress vessel growth. The assay plays an important role on detection of vessel formation by virtue of its low cost, no vivisection, and direct insight into vessel distribution. However, manual counting the $\boldsymbol{BCD}$ from a chicken chorioallantoic membrane image is very time-consuming and poor accuracy. It is important to develop a method automatically counting $\boldsymbol{BCD}$ from a chicken chorioallantoic membrane image for a biologist. In this paper, a Canny-based vessel detector is proposed to automatically detect the vessels from a chicken chorioallantoic membrane image. The Canny-based vessel detector automatically extract the vessels from from a chicken chorioallantoic membrane image and then calculate the $\boldsymbol{BCD}$ for the chicken chorioallantoic membrane image.

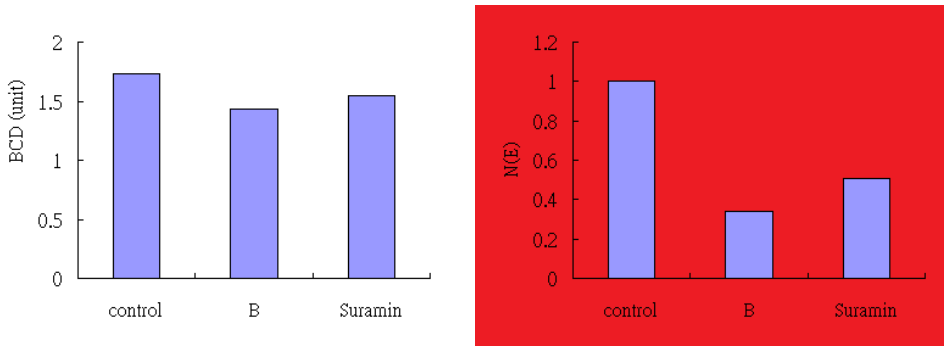

(a) $\boldsymbol{BCD}$ (b) $\boldsymbol{N(E)}$

FIGURE 3. The experimental $\boldsymbol{BCD}$ and $\boldsymbol{N(E)}$

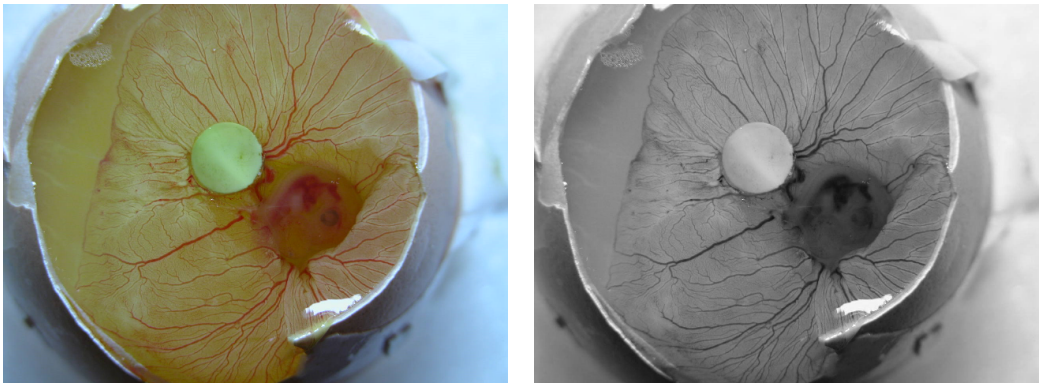

(a) Color image (b) G grey-level inage

FIGURE 4. Chiken chorioallantoic membrane image

2. **Canny-Based Vessel Detector.** Calculating the $\boldsymbol{BCD}$ is time-consuming. In this paper, the Canny-based vessel detector is proposed to calculate the $\boldsymbol{BCD}$ for a biologist. The Canny-based vessel detector can effectively segment the vessel from a color chicken chorioallantoic membrane image and then calculate the $\boldsymbol{BCD}$ the segmented vessel. Figure 5 demonstrates the framework of the Canny-based vessel detector. This section will describe it in details.

The Canny-based vessel detector considers the green channel of a color chicken chorioallantoic membrane image with RGB color channels to a gray-level image, and cut off the vessel from the gray-level image. Approximately locating vessel edges, known as hard edges by using the Canny edge detector method, we could recognize the pixels as vessels around the hard edges because the vessel color of the gray image usually is obscurer, and the standard direction change was higher than the one in the background. In this section, we will discuss more about the process of Canny-based vessel detector.

From the color chicken chorioallantoic membrane image, results showed that the yolk contained great quantity of G color component, but the vessel only contained minute, so among the RGB color components, G is the one that can distinguish the vessels and albumins. Therefore, Canny-based vessel detector can only preserve the G color component from the color image and integrate it into a gram image, G gray-level image. Figure 4(b) is the G gray-level image integrated from Figure 4(a), the color chicken chorioallantoic membrane image.

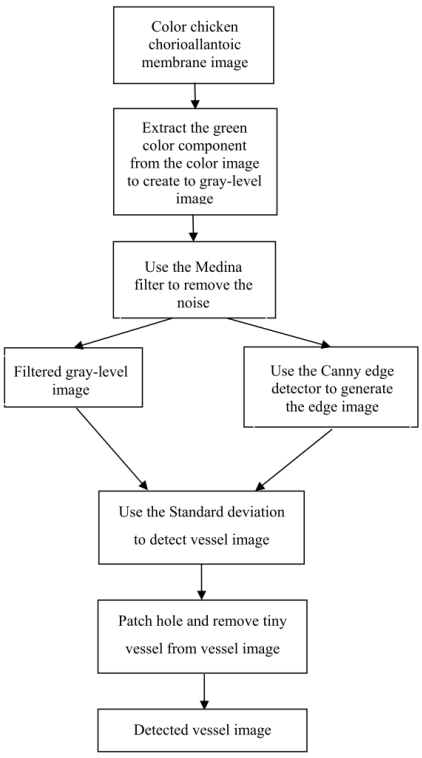

FIGURE 5. The framework of the Canny-based vessel detector

Canny-based vessel detector also adopted Median filter [10], the most effective miscellaneous articles eliminating technology, in order to clean the miscellaneous articles of the G gray-level image. Images usually can be interfered or contaminated and caused miscellaneous articles through filming, scanning, filing and delivering. These irrelevant miscellaneous articles should be eliminated beforehand because they usually disrupt the image process. Figure 6 is the result of Figure 4(b), G grey-level image, after the median filter process.

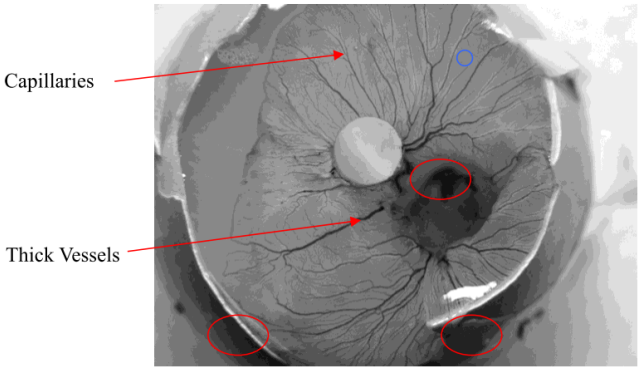

FIGURE 6. The G grey-level image processed by median filter

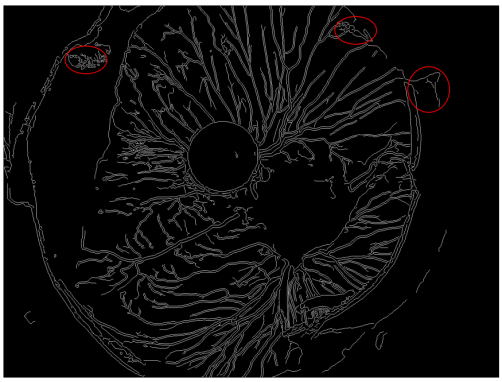

FIGURE 7. The edge pixels detected by Canny edge detector

We used the Canny edge detector [1], the most well-used and effective edge detecting method, to detect the vessel parts in G gray-level image. The noises, delicate lines, and the pixels on the edges of the object could cause false edge or generate a stripe rim line. The typical solvent is to set a threshold. The pixels that are lower a certain gradient of the threshold are assigned as the non-edged pixels, the other pixels are the edged pixels. However, it is an important research issue to automatically set up a proper threshold. Low value will generate many false edges; High value will omit many true edges. It is considerable to set up several threshold values. Canny edge detector took two values, the high one $\boldsymbol{T_h}$ and the low one $\boldsymbol{T_l}$, and scanned every pixel on the gradient image. When the pixel gradient value is higher/equal than to $\boldsymbol{T_h}$, it is the hard edge pixel; when the pixel is lower/equal than to $\boldsymbol{T_l}$, it is soft edge pixel, and the other pixels are non edge pixels.

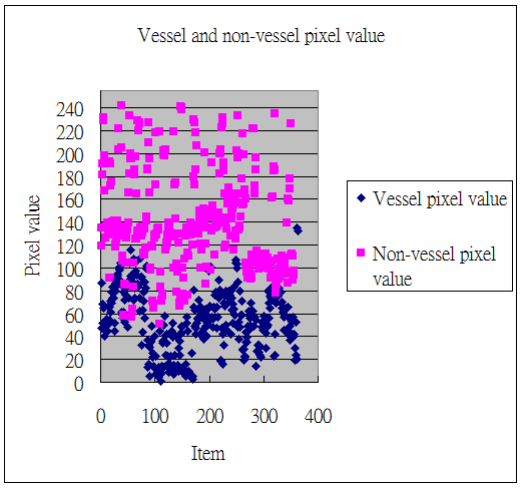

FIGURE 8. The colorful distribution of pixels on blood and non-blood vessels

Next, check every soft edge pixel. If it is next to the hard edge pixel, it is considered as a hard pixel. Mark every hard edge pixel as 1, the other pixel as ***0***. These ***0s*** and ***1s*** can generate a duality image. Some pixels around the edge pixels might be mistaken as hard edge pixels because of their high gradient value. Therefore, we should use the thinning technology to eliminate the hard edge pixels of the non true edge pixels from the duality image. Figure 7 is the duality image generated from Figure 6, the G-grey-level image, after Canny edge detector process. $\boldsymbol{T_l}$ and $\boldsymbol{T_h}$ values are ***0.05*** and ***0.015***. We named this duality image as edge image.

Canny edge detector can only detect the vessel edge because it decides edge pixels by the gradient values between pixels. It may mistake some inner shell membrane as vessels, as the red frame of Figure 7, and some true edge pixels as false edge pixels because of their low gradient values, which make breaks the rim line. All of these will affect the judgment of $\boldsymbol{BCD}$ for $\boldsymbol{BCD}$ can only test the complexity of vessel locus, not the one around the vessel edge. Canny-based vessel detector utilizes the pixel color in order to eliminate the non-vessel parts gained from the Canny edge detector since the color of vessels is different from the one of egg shells and membrane. Moreover, Canny-based vessel detector can decide vessel pixels by the following features: the vessel color is darker and the standard direction changes are stronger.

In this paper, we manually took $\boldsymbol{360}$ vessel and $\boldsymbol{360}$ non-vessel pixels from the four G grey-level images of chicken chorioallantoic membrane. In Figure 8, the blues spots represented vessel pixels, and the red ones represented non-vessel pixels. In the diagram, $\boldsymbol{X}$ axial showed the numbers of pixels. Figures 8 showed that most vessel pixel color values were below $\boldsymbol{140}$. Canny-based vessel detector related the edge pixels of the edge to the G grey-level image and only preserved the pixels color values that were below $\boldsymbol{140}$, named seed pixels, and then calculated their average color value $\overline{\boldsymbol{C_s}}$, and standard direction, $\overline{\boldsymbol{STD_s}}$.

We divided vessels into thick and micro vessels. Thick vessels were darker and their color standard directions were smaller. (with a smoother internal); On the other hand, the color and standard directions of micro vessels were bigger than thick vessels, as the indicated parts by red arrow in Figure 6. In G grey-level image, the pixels with the color values lower than $\overline{\boldsymbol{C_s}}$ were the thick vessel pixels and with the values between $\overline{\boldsymbol{C_s}}$ and $\boldsymbol{140}$ were micro vessels. However, the shadows of egg shells and embryos were also darker, shown by the red frame in Figure 6. From our observation, we still could use color standard direction to distinguish the difference between the internal lines of thick vessels from egg sells and embryos because the internal lines of thick vessels were more complicated.

Generally, the color value of micro vessels is lighter even though the lines are more complicated than the ones of thick vessels. Therefore, if the pixel value in G grey-level image was between $\overline{\boldsymbol{C_s}}$ and $\boldsymbol{140}$, the pixel might belong to micro vessels, so as the other non vessel pixel, as the blue frame indicated in Figure 6. We still could use the color standard direction to separate the differences since the lines around micro vessels were more complicated than non-vessel parts under normal situation.

There are two edges in a vessel, and the pixels between the edges were darker, and the other pixels outside the edges were lighter, as Figure 9. Canny-based vessel scanned every pixel of G grey-level image from top/down to left/right. If a pixel was near the seed pixel and also possessed the above mentioned features of thick vessels or micro vessels, it was considered as the vessel pixels.

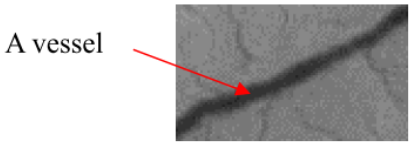

FIGURE 9. A part of vessel image

Let the pixel being scanned be $\boldsymbol{G(x,y)}$ and its color value be $\boldsymbol{C(x,y)}$, where $\boldsymbol{(x,y)}$ represents the coordinate of $\boldsymbol{G(x,y)}$ located on the image. If $\boldsymbol{G(x,y)}$ is a seed pixel, then run the following algorithm where the contents in brackets are comments. Due to the changes of features related with capillaries in different image, $\boldsymbol{THR}$ and $\boldsymbol{W}$ are

custom parameters, so the limit condition of the standard deviation is set $\boldsymbol{STD_B(x,y) \geq (\overline{STD_s} \times W)}$. Suppose mn is a small window around $\boldsymbol{G(x,y)}$ and $\boldsymbol{V}$ is the result, which is a binary image where the vessel pixels are marked as *1*; Otherwise, marked as *0*. Figure 10 shows the binary image $\boldsymbol{V}$ from Figure 7 by running the algorithm.

$\overline{G_l} = \frac{\sum_{i=0}^{4} G(x-i,y)}{5}$

$\overline{G_r} = \frac{\sum_{i=2}^{6} G(x+i,y)}{5}$.

If $\overline{C_l} > \overline{C_r}$ **then** {indicating that $\boldsymbol{P}$ is a pixel on the left edge}

$\boldsymbol{G_B = \frac{1}{m \times n} \sum_{i=-\lfloor \frac{m}{2} \rfloor}^{\lfloor \frac{m}{2} \rfloor} \sum_{i=-\lfloor \frac{n}{2} \rfloor}^{\lfloor \frac{n}{2} \rfloor} G(x+i, y+j)}$

$\boldsymbol{STD_B(x,y) = \sqrt{\frac{1}{m \times n} \sum_{i=-\lfloor m/2 \rfloor}^{\lfloor m/2 \rfloor} \sum_{j=-\lfloor n/2 \rfloor}^{\lfloor n/2 \rfloor} (G(x+i, t+j) - \overline{G_B})^2}}$

If $(\boldsymbol{C(x,y) \leqq \overline{C_s}}$ **and** $\boldsymbol{STD_B(x,y) > THR})$ **or** {check if it is thick}

$(\boldsymbol{\overline{C_s} < C(x,y) \leqq 140}$ **and** $\boldsymbol{STD_B(x,y) \geq (\overline{STD_s} \times W))}$ **then** {check if it is thin}

$\boldsymbol{V(x,y) = 1}$ {blood vessels}

Set $\boldsymbol{G(x+1,y)}$ to be a seed pixel

Else

$\boldsymbol{V(x,y) = 0}$ {non-blood vessels}

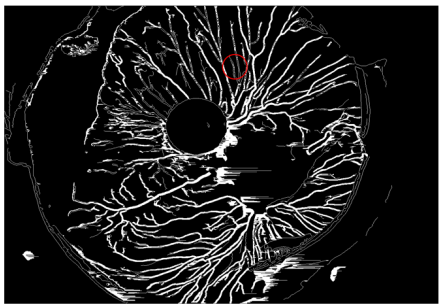

FIGURE 10. A vessel image $(\boldsymbol{THR = 0.5, W = 0.25})$

Some vessel pixels might be unable to extend and be discontinued during this process because of the noises, as the red circle in Figure 10. Hence, Canny-based vessel detector repair the image $\boldsymbol{V}$ by scanning every pixel from left to right and correct every scanned pixel $\boldsymbol{V(x,y)}$. If the pixels between $\boldsymbol{V(x,y-1)}$ and $\boldsymbol{V(x,y+N)}$; $\boldsymbol{V(x,y-1)}$ and $\boldsymbol{V(x,y+(N-1)}$; $\boldsymbol{V(x,y-1)}$ and $\boldsymbol{V(x,y+2)}$; $\boldsymbol{V(x,y-1)}$ and $\boldsymbol{V(x,y+1)}$; $\boldsymbol{V(x,y+1)}$ and $\boldsymbol{V(x,y-N)}$; $\boldsymbol{V(x,y+1)}$ and $\boldsymbol{V(x,y-(N+1)}$; $\boldsymbol{V(x,y+1)}$ and $\boldsymbol{V(x,y-2)}$; and $\boldsymbol{V(x,y+1)}$ and $\boldsymbol{V(x,y-1)}$ are all vessel pixels, then set all pixels located in the regions of these coordinates to be vessel pixels. $\boldsymbol{N}$ is the diameter of patched holes.

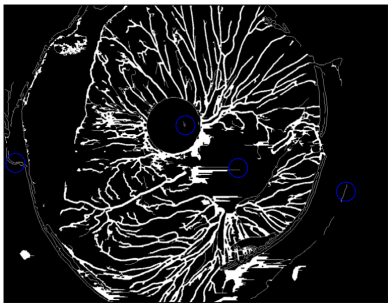

FIGURE 11. The result from Figure 10 with hole patching $(\boldsymbol{N = 3})$

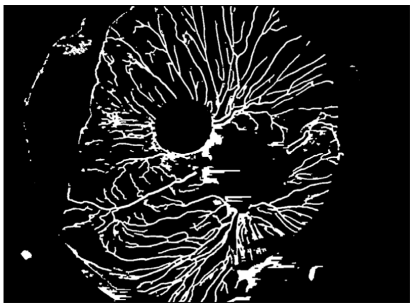

FIGURE 12. The image without the part with the width of two pixels

Similarly, scan every pixel once again in top-down fashion. If the pixels between $\boldsymbol{V(x-1,y)}$ and $\boldsymbol{V(x+N,y)}$; $\boldsymbol{V(x-1,y)}$ and $\boldsymbol{V(x+(N-1),y)}$; $\boldsymbol{V(x-1,y)}$ and $\boldsymbol{V(x+2,y)}$; $\boldsymbol{V(x-1,y)}$ and $\boldsymbol{V(x+1,y)}$; $\boldsymbol{V(x+1,y)}$ and $\boldsymbol{V(x-N,y)}$; $\boldsymbol{V(x+1,y)}$ and $\boldsymbol{V(x-(N-1),y)}$; $\boldsymbol{V(x+1,y)}$ and $\boldsymbol{V(x-2,y)}$; $\boldsymbol{V(x+1,y)}$ and $\boldsymbol{V(x-1,y)}$ are all vessel pixels, then set all pixels located in the regions of these coordinates to be vessel pixels. Figure 11 illustrates the result from Figure 10 by running the above procedures.

Generally, it is unlikely that there are two pixels on the width of a vessel, such as the part closed in blue circles. As a result, the part in $\boldsymbol{V}$ with the width of two pixels is removed by Canny-based vessel detector. Analogously, every pixel $\boldsymbol{V(x,y)}$ is scanned from left to right. If the pixels between $\boldsymbol{V(x,y-1)}$ and $\boldsymbol{V(x,y+2)}$; $\boldsymbol{V(x,y-1)}$ and $\boldsymbol{V(x,y+1)}$; $\boldsymbol{V(x,y+1)}$ and $\boldsymbol{V(x,y-2)}$; and $\boldsymbol{V(x,y+1)}$ and $\boldsymbol{V(x,y-1)}$ are all vessel pixels, then set all pixels located in the regions of these coordinates to be vessel pixels. The same is in $\boldsymbol{V(x-1,y)}$ and $\boldsymbol{V(x+2,y)}$; $\boldsymbol{V(x-1,y)}$ and $\boldsymbol{V(x+1,y)}$; $\boldsymbol{V(x+1,y)}$ and $\boldsymbol{V(x-2,y)}$; $\boldsymbol{V(x+1,y)}$ and $\boldsymbol{V(x-1,y)}$. The processed results from Figure 11 are shown in Figure 11.

3. **Experimental Results and Discussion.** The purpose of this section is to investigate the performances of Canny-based vessel detector by experiments. In these experiments, the color images "**B1**", "**B2**", "**B3**", and "**B4**," shown in in Figure 13, are used as the testing images each of which consists of $\boldsymbol{1280 \times 960}$ pixels. In these experiments, the variables $\boldsymbol{m, n, T_l}$, and $\boldsymbol{T_h}$ are set to be $\boldsymbol{3,\ 3,\ 0.05}$, and $\boldsymbol{0.15}$. The Canny-based vessel detector first utilizes Canny edge detector to detect the edges on "**B1**", "**B2**", "**B3**", and "**B4**". Figure 13 shows the images from **B1**$\sim$**4** with the processing of Canny edge detector.

Canny-based vessel uses the value of color with combination of respective $\boldsymbol{THR}$ and $\boldsymbol{W}$ to differentiate thick vessels from thin ones. In the experiments, we will discuss respectively the influence of different $\boldsymbol{THR}$ and $\boldsymbol{W}$ on the detection ability of Canny-based vessel detector. In order to highlight the influence of respective $\boldsymbol{THR}$ and $\boldsymbol{W}$ on thick and thin vessels, capillaries will not be processed on discussing about the influence

of different ***THR*** on thick vessels while thick vessels will not be processed on discussing about the influence of different ***W*** on capillaries.

At first, the influence of different ***THR*** on thick vessels is tested, as shown in Figure 15, showing the affection of different ***THR, 0.1, 0.3, 0.5*** and ***0.7***, on thick vessels on **B1** and **B2**. With Figures 15 (a)-(d), we can find that it is unable to differentiate the pixels of non-blood vessels from those of blood vessels, e.g., the regions closed in red circles on Figures 15 (a)-(d). With more ***THR***, the less probability of misjudgment on the pixels of non-blood vessels comes, e.g., the regions closed in red circles on Figures 15 (e)-(h). Unfortunately, it occurred that a few pixels of vessels are misjudged as the pixels of no-blood vessels, such as the regions closed in blue circles on Figures 15 (e)-(h), resulting in the situation that the probability of misjudgment between the pixels of non-blood vessels and blood vessels is contrary to ***THR***. In the following, the influence of different ***W*** on capillaries will be discussed, as shown in Figure 16, illustrating the influence of different ***W, 0.15, 0.2, 0.25***, and ***0.3***, on capillaries on **B1** and **B2**.

In Figures 16 (a)-(h), it is illustrated that the separation between the pixels of non-blood vessels and blood vessels cannot be done effectively, such as the regions closed in red circles on Figures 16 (a)-(d), on the conditions that $W \leqq 0.2$. The situation that the pixels of non-blood vessels misjudged as those of blood vessels are improving with great ***W***, such as the regions closed in red circles on Figures 16 (e)-(h).

With the previous experimental results, it is known that Canny-based vessel detector can obtain the best solution if $THR = 0.5$, $W = 0.25$. Figure 17 shows the vessels on the test images obtained by the Canny-based vessel detector, where ***THR=0.5*** and ***W=0.25***.

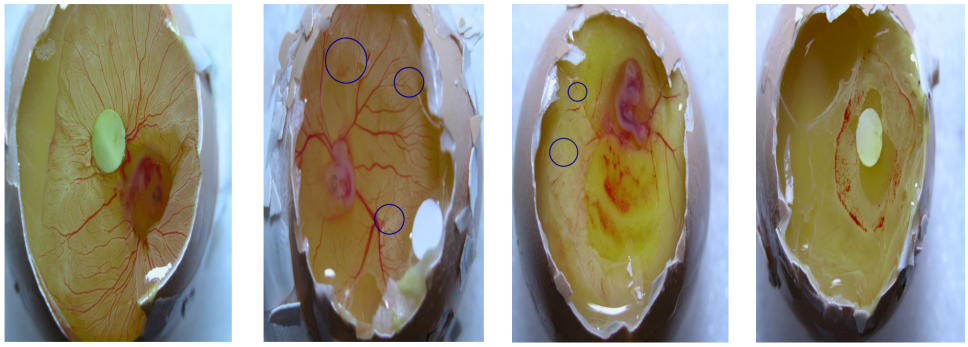

(a) **B1** (b) **B2** (c) **B3** (d) **B4**

FIGURE 13. The test images

(a) **B1** (b) **B2** (c) **B3** (d) **B4**

FIGURE 14. The edges on test images obtained by Canny edge detector

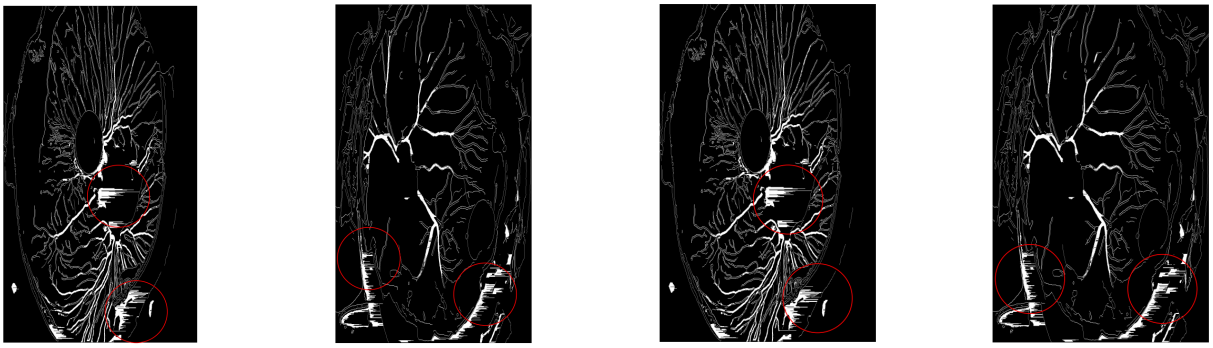

(a) $\boldsymbol{THR = 0.1}$ for **B1** (b) $\boldsymbol{THR = 0.1}$ for **B2** (c) $\boldsymbol{THR = 0.3}$ for **B1** (d) $\boldsymbol{THR = 0.3}$ for **B2**

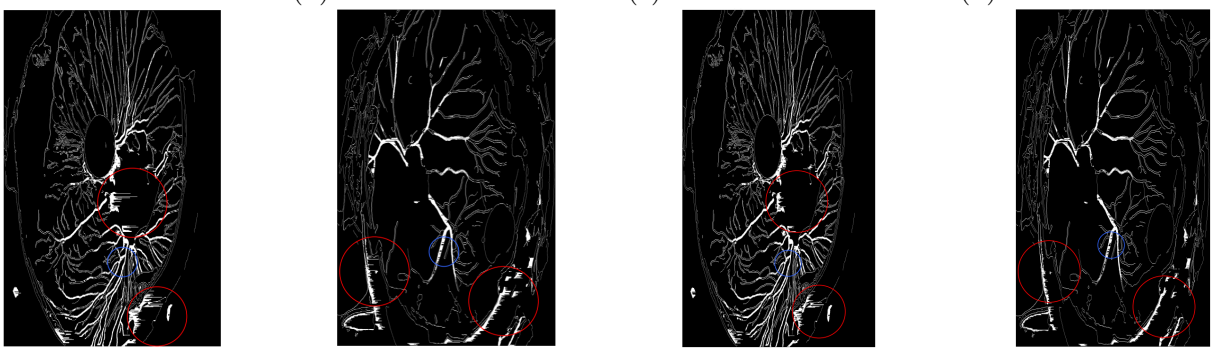

(e) $\boldsymbol{THR = 0.5}$ for **B1** (f) $\boldsymbol{THR = 0.5}$ for **B2** (g) $\boldsymbol{THR = 0.7}$ for **B1** (h) $\boldsymbol{THR = 0.7}$ for **B2**

FIGURE 15. Variable $\boldsymbol{THR}$ for **B1** and **B2**

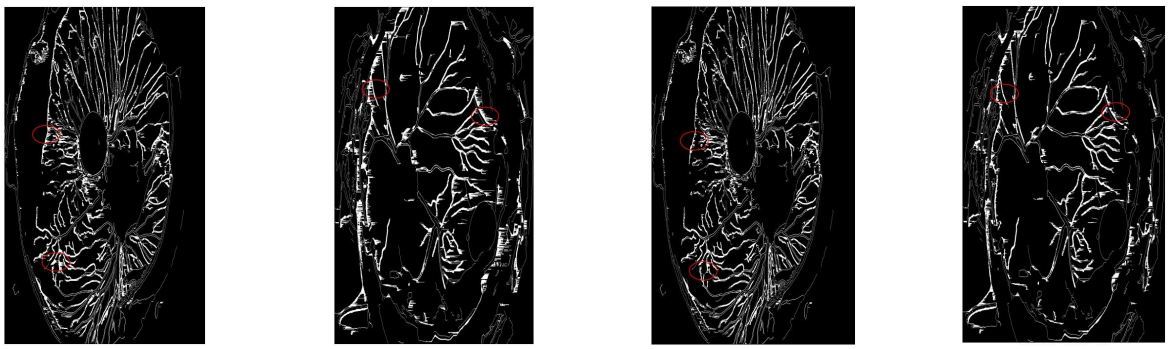

(a) $\boldsymbol{W = 0.15}$ for **B1** (b) $\boldsymbol{W = 0.15}$ for **B2** (c) $\boldsymbol{W = 0.2}$ for **B1** (d) $\boldsymbol{W = 0.2}$ for **B2**

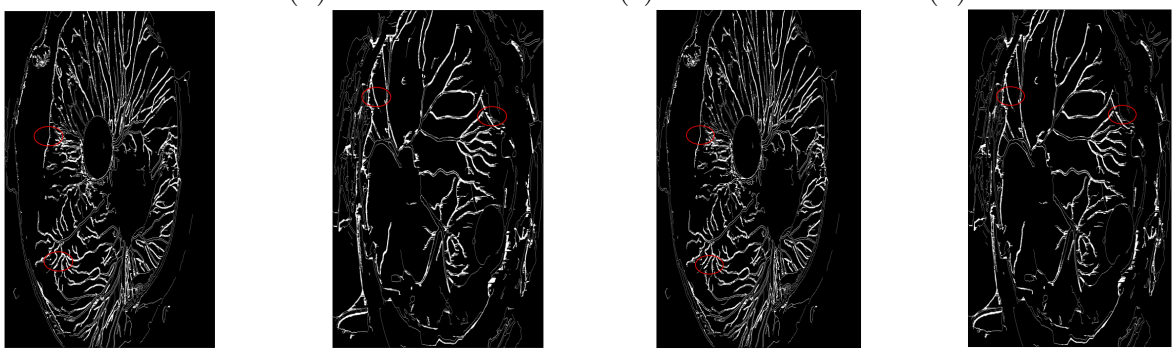

(e) $\boldsymbol{W = 0.25}$ for **B1** (f) $\boldsymbol{W = 0.25}$ for **B2** (g) $\boldsymbol{W = 0.3}$ for **B1** (h) $\boldsymbol{W = 0.3}$ for **B2**

FIGURE 16. Variable $\boldsymbol{W}$ for **B1** and **B2**

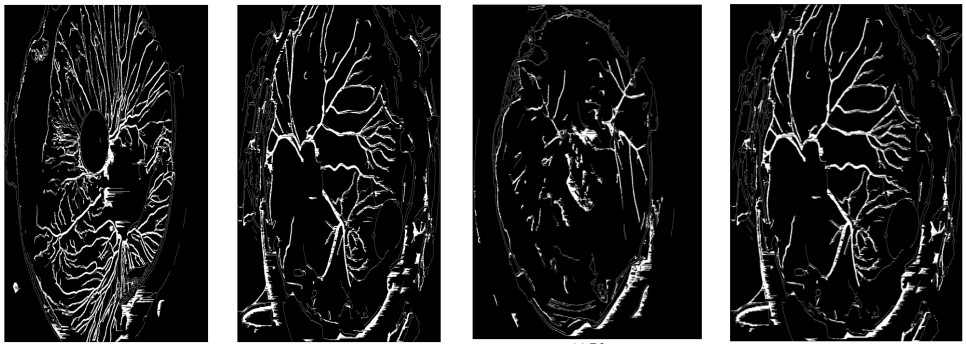

(a) **B1** (b) **B2** (c) **B3** (d) **B4**

FIGURE 17. The vessels on the test images obtained by the Canny-based vessel detector $(\boldsymbol{THR = 0.5, W = 0.25})$

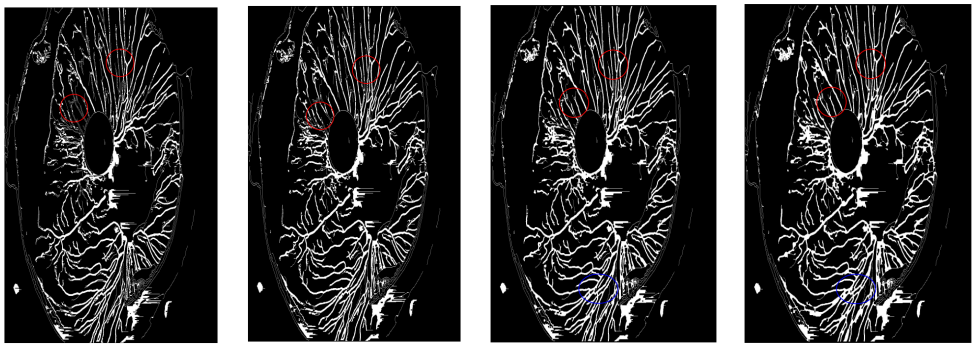

(a) $\boldsymbol{N = 1}$ (b) $\boldsymbol{N = 2}$ (c) $\boldsymbol{N = 3}$ (d) $\boldsymbol{N = 5}$

FIGURE 18. Variable $\boldsymbol{N}$ for **B1**

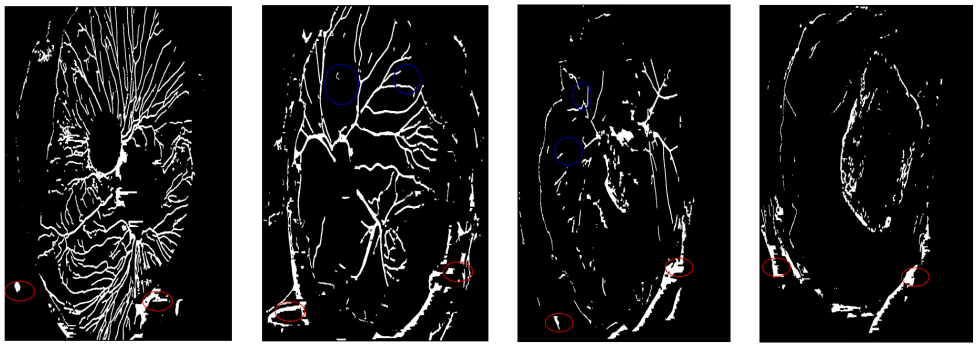

(a) **B1** (b) **B2** (c) **B3** (d) **B4**

FIGURE 19. The vessels on the test images obtained by the Canny-based vessel detector $(\boldsymbol{THR = 0.5, W = 0.25, N = 3})$

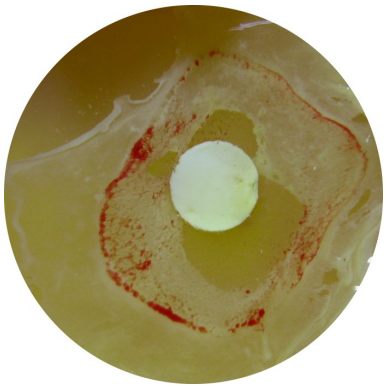

FIGURE 20. The part of vessels inside the shell on **B4**

In the following experiment, we will discuss the influence of different N on the process that Canny-based vessel detector are patching holes. The results of **B1** with N, which is equal to ***1, 2, 3***, and ***4***, are shown in Figure 17. If $\boldsymbol{N \leqq 2}$, it is shown that there are a part of vessel pixels whose holes patching failed, such as the regions closed in red circles on Figures 18 (a) and (b). The above question is enhanced with great N, but the mix of two vessels, very closed to each other is induced, e.g., the regions closed in blue circles on Figures 18 (c) and (d). The level of mix caused by two closed vessels will become more serious with greater N.

Figures 15 to 19 obtained in the experiments show that the Canny-based vessel detector can work best while $\boldsymbol{N = 5}$. Figure 19 displays the extracted vessels on the test images obtained by the Canny-based vessel detector, where $\boldsymbol{THR = 0.5, W = 0.25}$, and $\boldsymbol{N = 5}$.

The results by using Canny-based vessel detector on the color chicken chorioallantoic membrane images are the binary images, as shown in Figure 19 where "1" and "0" indicate vessel pixel and non-blood vessel pixel, respectively. We take as an example the part circled in blue in Figures 13 (b) and (c), and Figures 19 (b) and (c). It is depicted that slightness and fuzz of vessels cause Canny edge detection not to work properly, making vessels undetectable or discontinuous.

There are a part of the pixels on non-blood vessels, which are misjudged as the pixels on blood vessels, such as, the regions closed in red circles on Figure 20. With comparison between the red regions in Figure 19 and the corresponding regions in Figure 16, we can find that the misjudged locations almost lie around the egg shell or shadow. Nonetheless, we are mainly interested in the part of vessels, so the only regions, which need to be reserved, are the areas inside the shell, not the shell included, as shown in Figure 20. In the manner, we can solve the above question.

4. **Conclusions.** The process of vessel growth, while is called Angiogenesis and is influenced by active and passive factors, such as Growth factors, Cytokines, Proteolysis, etc. Without balance on Angiogenesis, the abnormal phenomenon of Angiogenesis will be produced. The medical studies showed that the distribution and density of vessel generation can be used to analyze whether a person suffers from Cancer, Rheumatoid arthritis, Diabetes, Arteriosclerosis or so on. Hence, it is worth studying how to get blood vessel segmentation from the images of organs and further analyze it.

In this paper, we present a method, called Canny-based vessel detector, to automatically examine the part of vessels on chicken chorioallantoic membrane images. In the first place, the approach is to detect the edges of vessels and then mark the vessel pixels precisely by means of the pixel colors and their standard deviation. Nonetheless, most of vessels can be detected by our method on the whole. Future work will be focused on the detection of tiny vessels.

REFERENCES

[1] J. Canny, A computational approach to edge detection, *IEEE Transactions on Pattern Analysis and Machine Intelligence*, vol.8, no. 6, pp.679-698, 1986.

[2] P. Carmeliet, Angiogenesis in life, disease and medicine, *Nature Insight Angiogenesis*, vol.438, no. 438, pp.932-936, 2005.

[3] I.J. Fidler, and L.M. Ellis, The implications of angiogenesis for the biology and therapy of cancer metastasis, *Cell*, vol.79, no.2, pp.185-188, 1994.

[4] J. Folkman, Tumor angiogenesis: therapeutic implications, *New England Journal of Medicine*, vol.285, no. 21, pp. 1182-1186, 1971.

[5] J. Folkman, and C. Haudenschild, Angiogenesis in vitro, *Nature*, vol. 288 , no. 5791, pp. 551-556, 1980.

[6] J. Folkman, What is the role of endothelial cells in angiogenesis?, *Laboratory Investigation*, vol.51, no. 6, pp. 601-604, 1984.
[7] J. Folkman, and Y. Shing, Angiogenesis, *Journal of Biological Chemistry*, vol. 267, no. 16, pp.10931-10934, 1992.
[8] M. A. Gimbrone, S. B. Leapman, R. S. Cotran, and J. Folkman, Tumor dormancy in vivo by prevention of neovascularization, *Journal of Experimental Medicine*, vol. 136, no. 2, pp. 261-276, 1972.
[9] A.J. Hayes, L. Y. Li, and M. E. Lippman, Antvascular therapy: a new approach to cancer treatment, *British Medical Journal*, vol. 318, no.7187, pp. 853-856, 1999.
[10] A. K. Jain, Fundamentals of digital image processing, *Prentice-Hall*, Englewood Cliffs, N. J., 1989.
[11] R. Kraft, Fractals and Dimensions, *HTTP-Protocol at www.weihenstephan.de*, 1995.
[12] F. Rastinejad, P. J. Polverini, and N. P. Bouck, Regulation of the activity of a new inhibitor of angiogenesis by a cancer suppressor gene, *Cell*, vol. 56, no. 3, pp. 345-355, 1989.
[13] B. R. Zetter, Angiogenesis and tumor metastasis, *Annual Review of Medicine*, vol. 49, no. 1407, pp. 407-424, 1998.